Green Chemistry

Cutting-edge research for a greener sustainable future

Accepted Manuscript

Green
Chemistry

Cutting-edge research for a greener sustainable future

rsc.li/greenchem

Volume 20
Number 9
7 May 2018
Pages 1919-2160

ISSN 1463-9262

ROYAL SOCIETY
OF CHEMISTRY

PAPER
Paul T. Anastas *et al.*
The Green ChemisTREE: 20 years after taking root with the 12 principles

ROYAL SOCIETY
OF **CHEMISTRY**

rsc.li/greenchem

Deep eutectic solvent-based microextraction system for simultaneous lignocellulose fractionation and furfural production

Liu Liu, Qianwei Li, Caixia Wan*

Department of Chemical and Biomedical Engineering, University of Missouri, 1406 Rollins Street, Columbia, MO, USA 65211

* Corresponding author: Tel: +1 573 884 7882, Email: wanca@missouri.edu

Abstract

A biomass conversion process with microextraction system was developed for simultaneous lignocellulose fractionation and conversion. The liquid-liquid biphasic platform was composed of deep eutectic solvent (DES) (polyethylene glycol:oxalic acid) and methyl isobutyl ketone (MIBK). Microemulsion (O/W) was formed with constant stirring and stabilized by sodium salt crystal, which also acted as an interphase catalyst to enhance furfural yields. Furfural was continuously extracted into MIBK after being formed in the DES. The highest furfural yield of 76.5% was obtained when the reaction was conducted at 150 °C for 60 min at the presence of 12.3 wt% NaCl. The extracted lignin was functionalized with polyethylene glycol, with substantial retention of native structure of lignin. The pulp also showed high enzymatic digestibility of cellulose. This work demonstrated the role of salt crystals in stabilizing Pickering emulsion for microextraction and its function in simultaneous biomass fractionation and conversion for high-value platform chemicals, paving the way toward sustainable biorefineries.

Keywords: Biomass fractionation; Furfural; Biphasic system; Microextraction

1. Introduction

Furfural is one of top value-added platform chemicals derived from biomass[1] and has a broad spectrum of industrial applications such as solvents, plastics, and pharmaceuticals.[2, 3] Furfural is produced from pentose, with xylan-rich lignocellulosic biomass almost as an exclusive feedstock as there is no synthetic route available for petroleum source to furfural.[3, 4] Two main steps are involved in furfural production, i.e., xylan hydrolysis into xylose followed by xylose dehydration into furfural.[5] The prevailing furfural production technology is primarily based on mineral acid-catalyzed reaction systems. However, such process is energy intensive, generates large quantities of solid and liquid waste, and has low furfural yields. With growing market for furfural, it is important to address those drawbacks by developing more cost-effective processes to promote sustainable growth of furfural industry.

Solvent systems based on green chemistry principles have been explored for furfural production. Deep eutectic solvents (DESs) composed of hydrogen bond acceptor (HBA) and hydrogen bond donor (HBD) have been extensively explored for biomass pretreatment. DESs, with most constituents being renewable, low-cost, and non-hazardous, can function as both reaction media and catalysts, providing an economic, environmentally friendly, and versatile alternative to traditional mineral acid-based catalysts. This makes DES a promising choice for fractionation of lignocellulose and catalytic conversion of xylan into furfural. Especially, polyol-based DESs were reported to effective for dissolving lignin from biomass due to strong interactions between hydroxyl groups on polyols and those on lignin, leading to improved cellulase accessibility to cellulose pulp. Thus, such DESs represent a new class of designer solvents with unique surface tension and thermodynamic properties.[6]

Compared to DESs typically based on quaternary ammonium salts, the incorporation of polyols in DES formulations contributes to enhanced stabilization of intermediates in biomass

pretreatment. Liu et al.[7] developed a ternary DES by adding ethylene glycol (EG) in choline chloride (ChCl):oxalic acid (OA). The presence of EG was reported to stabilize carbocation and prevent the breakdown of β-O-4 linkages during pretreatment, leading to higher lignin extraction efficiency and greater selectivity of aromatic monomers via depolymerization. Xue et al.[8] designed ChCl:glycerol:polyethylene glycol (PEG) ternary DESs with excellent lignin dissolving ability. Polyols composed of glycerol/PEG were believed to participate in lignin liquefaction with intermolecular hydrogen bonding. Additionally, polyols were found to promote furfural conversion and slow down its degradation during prolonged reaction times.[9] Therefore, the rational design of polyol-based DESs capable of stabilizing xylose and other degradation intermediates will provide effective strategies for enhancing the efficiency of biomass fractionation and furfural production.

Furfural tends to degrade rapidly through resinization and self-condensation once synthesized, resulting in low yields. *In situ* extraction using a biphasic system is an effective way to minimize degradation and enhance furfural production. By introducing an organic phase into the solvent system, furfural can be continuously transferred to the organic phase, thereby reducing its concentration in the aqueous phase and minimizing degradation. Cheng et al.[10] developed a novel DES/γ-Valerolactone (GVL) biphasic system based on DES (ChCl:OA, ChCl:*p*-toluenesulfonic acid) and GVL and achieved 68.6% furfural yield. Emmanuel et al.[11] developed a catalytic system comprising AlCl₃/LiCl/NaCl in H₂O/MIBK biphasic media, achieving production of furfural and hydroxymethylfurfural from corrugated boxes with maximum yields of 51 % and 98 % at 160 °C and 40 min. Gabriel et al.[12] reported furfural synthesis with a high yield of 77% in a biphasic system (butyl acetate and saturated NaCl solution) with the assistance of microwave at 160 ºC for 10 min. Despite the advantages of biphasic systems, they has inherent mass transfer limitation associated with two phases.[13] This transfer barrier ascribing to the limited interfacial contact can lead to rehydration and by-product formation.[14] To address these challenges, a biphasic system based on

Pickering emulsion looks promising for effective fractionation process. The presence of the emulsion micelle has been shown to significantly enhance mass transfer at the interface in a binary solvent system.[15]

In this study, DESs composed of PEG and oxalic acid (OA) were synthesized to enable biomass fractionation and simultaneous conversion of xylan to furfural. The addition of NaCl triggered the formation of Pickering emulsion. Pretreatment effectiveness was evaluated by analyzing chemical composition and enzymatic digestibility of pulp. Lignin extracted via biphasic reaction system was characterized for detailed chemistry. The effects of key reaction parameters, including $NaCl/H_2O$, reaction temperature, and time, on furfural yields and selectivity were also studied. The mechanism involved in lignocellulose fractionation and catalytic synthesis of furfural at the interphase was also proposed.

2. Materials and Methods

2.1 Materials

Switchgrass collected from the South Farm in the University of Missouri was air-dried and ground through 40-mesh screen. It was mainly composed of 33.91 wt% cellulose, 23.45 wt% xylan, and 19.54 wt% lignin. Cellic® CTec2 and HTec2 were kindly provided by Novozyme (Franklinton, NC, USA). All the chemicals were of analytical grade and purchased from Fisher Scientific (Heysham, Lancashire, UK).

2.2 Biomass pretreatment

DESs were synthesized by mixing PEG400 and OA with the mole fraction of PEG (average Mn 400) ranging from 0 to 1 at 80 ºC until forming a clear and transparent liquid. Biphasic solvent systems were prepared by mixing DES, MIBK, H_2O or NaCl solution (25 wt% NaCl content) with varied mass ratios specified in Table S1. In a typical run of pretreatment, 2.0 g of air-dried

switchgrass (9.5% moisture content) was mixed with 40.0 g of biphasic solvent in a 100 mL hydrothermal reactor. The reactor was heated to different temperatures (i.e., 130, 140, 150, 160 ℃) for 60 min, or heated at 150 ℃ for varying durations (i.e., 20, 40, 60, 80, 100 min) with constant magnetic stirring at 800 rpm. Thereafter, the reactor was cooled down to room temperature followed by adding 100 mL of water. The solid residues and liquid were collected separately by vacuum filtration. The filtrate (i.e., liquid fraction) was further separated into aqueous and organic phases in a separatory funnel and each phase was subjected to furfural analysis. Lignin was recovered by washing the solid residues with aqueous acetone (60%, w/w) followed by acetone removal and then freeze-dried. The pulp resulting from lignin removal was subjected to enzymatic hydrolysis as detailed in the Supporting Information.

2.3 Characterization

The concentrations of furfural, xylose, and glucose were determined using HPLC (Agilent 1100 series) equipped with diode array detector (DAD, 268 nm) and refractive index detector (RID). Aminex HPX-87H column was used for the analysis of furfural in aqueous phase and monomeric sugars (i.e., glucose, xylose), and the mobile phase was 5 mM sulfuric acid, eluting at 0.6 mL/min. The temperatures of column and RID were maintained at 65 ℃ and 40 ℃, respectively. Phenomenex Luna C18(2) column was used to analyze furfural in organic phase, and the mobile phase was methanol/water (20/80, v/v), eluting at 0.8 mL/min at 30 ℃. All the samples were filtered through 0.22 μm Nylon syringe filter prior to HPLC analysis.

Furfural yield, xylose conversion, furfural selectivity, and glucose conversion were calculated following Equations 1-4. Lignin and cellulose contents in switchgrass were determined following NREL Laboratory Analytical Procedure as detailed in the Supporting Information.[16]

$$Furfural\ yield\ (\%) = \frac{Moles\ of\ furfural\ produced}{Moles\ of\ xylose\ in\ raw\ switchgrass} \times 100\% \qquad (1)$$

$$\textit{Xylose conversion } (\%) = \frac{\textit{Moles of xylose converted}}{\textit{Moles of xylose in raw switchgrass}} \times 100\% \qquad (2)$$

$$\textit{Furfural selectivity } (\%) = \frac{\textit{Moles of furfural produced}}{\textit{Moles of xylose converted}} \times 100\% \qquad (3)$$

$$\textit{Glucose conversion } (\%) = \frac{\textit{Moles of glucose converted}}{\textit{Moles of glucose in raw switchgrass}} \times 100\% \qquad (4)$$

FTIR spectra were acquired on Nicolet 4700 FTIR Spectrometer attached with ATR. The samples were scanned from 500–4000 cm^{-1} range at room temperature with a resolution of 4 cm^{-1} and accumulation of 64 scans. ^{1}H-^{13}C HSQC spectrum was acquired on Bruker Advance III 600 MHz NMR Spectrometer. The analysis was carried out at 323 K with acquisition parameters as follows: "Hsqcedetgp" pulse program with spectral widths of 9014 Hz (from 15 to 0 ppm) and 25635 Hz (from 170 to 0 ppm) for the ^{1}H- and ^{13}C-dimensions; size of FID set as 1024 (F2) and 256 (F1) with the number of scans of 32. The NMR spectrum was processed using MestReNova version 15.0.0.

Rheological properties were analysed using Anton Parr SmartPave 102 rotational rheometer equipped with 25 mm plate geometry. Static viscosity was measured at a sheer rate of 10 s^{-1}. Dynamic properties were determined in the frequency sweep mode with angular frequency ranging from 0.1 to 100 rad/s.

Thermal properties were analyzed using TA Differential Scanning Calorimetry (DSC) Q20. Melting points were determined under 20 mL/min nitrogen flow. Samples (6~8 mg) were sealed in aluminum pans, and the temperature was ramped to 80 ℃ at a heating rate of 10 ℃/min, and equilibrated at that temperature for 5 min. Afterwards, the samples were cooled down to -70 ℃ at a cooling rate of 5 ℃/min, held at the same temperature for 5 min, and finally reheated to 80 ℃ at a heating rate of 5 ℃/min. The melting enthalpy was integrated from the endothermic peak area from the second heating cycle using the TA Universal Analysis software.

3. Results and discussion

3.1 Hydrogen bond formation in DES

The hydrogen bonding interactions in DES are the main driving force for biomass fractionation.[17] These interactions indicate the reactivity of biomass pretreatment system. The hydrogen bond network in DES was characterized for thermal properties, rheological properties, and functional groups. The melting point of pure PEG 400 is -10.37 ℃ (Figure 1a), while that of OA is 98 ℃. By varying the molar fraction of PEG (χ_{PEG}), the DESs exhibited a phase transition from solid to liquid at room temperature (Figure 1b), along with the corresponding changes in melting points. The melting points of PEG:OA mixtures were lower than those of individual components. The eutectic point of DES with χ_{PEG} of 0.5 had the minimum melting point of -63.94 ℃, which was much lower than that of DESs reported previously.[18] This decrease in melting point was associated with the formation of hydrogen bonding between PEG and OA, which reduced lattice energy of eutectic solvent.[19] The lowest melting enthalpy (5.05 J/g) was also observed at the eutectic point (Table S2), indicating a shorter range and weaker configuration of hydrogen bonds compared to non-eutectic points on the phase diagram. This finding agreed with previously reported trends in surface tension.[20] Such a unique structural feature allowed DES to easily disrupt internal hydrogen bonds and form competitive hydrogen bonds with substances, thereby improving their dissolving capabilities.[21] Considering strong potential for biomass fractionation, DES (χ_{PEG} = 0.5) was thus used for the proposed biomass pretreatment.

The viscoelasticity of DES differed notably from that of pure PEG, demonstrating alterations of the solvent structure (Figure 1c and d). For PEG (Figure 1c), the initial loss modulus (G") was higher than the storage modulus (G'). Although both G' and G" increased with angular frequency, G" remained consistently higher. The dominance of G" indicated that PEG 400 exhibited more viscous behavior than elastic one under applied deformation or stress. In contrast, PEG:OA initially

showed G' higher than G" (Figure 1d). The crossover of G' and G" at increasing frequencies suggested that the DES behaved like a weak gel with entangled polymer chains, indicative of a topological network.[22] This behavior validated the presence of strong hydrogen bonding, which remained highly crosslinked at low shear force but became vulnerable at high shear force. At lower frequencies (<4 rad/s), DES exhibited more crosslinked structures, leading to the dominance of elastic behavior (G'>G"). However, at higher frequencies (>4 rad/s), part of hydrogen bonds in the DES was disrupted, resulting in dominant viscous behavior (G">G').

The formation of hydrogen bonds between PEG and OA was further investigated by FTIR to gain deeper structural insights. In Figure 1e, the FITR spectrum of PEG showed peaks at 3447 cm^{-1} for O–H stretching (hydroxyl), 2869 cm^{-1} for the C−H stretching of methylene, and 1103 cm^{-1} for C–O stretching (ether). After PEG was combined with OA to form DES (χ_{PEG}=0.5), the O–H stretching vibration peak around 3447 cm^{-1} became broader, indicating the formation of hydrogen bonds. The blue-shifting of C–H to 2876 cm^{-1} was inferably caused by the strong repulsion when approaching OA, inducing electron density redistribution within the pair of C–H (from PEG)···O (from OA) hydrogen bonding.[23, 24] The formation of hydrogen bond also accounted for the red-shifting of C–O stretching absorption peak to 1099 cm^{-1}, possibly originating from the attraction between protons (H–OOC− from OA) and HBA (the C–O from PEG).[25]

Adding water is necessary to address mass transfer limitation caused by the high viscosity of DES (215.17 mPa·s, 3.4 times that of pure PEG, Table S3) in biomass fractionation.[26] However, the hydrogen bond formation in DES was sensitive to water content, as indicated by the high correlation between solvent viscosity and intermolecular interaction. To evaluate the hydration effect on this hydrogen-bond-driven network structure of DES, 40% deuterated water (D$_2$O) was added. As shown in Figure 1f, after adding D$_2$O, the O–H band was red-shifted from 3446 to 3435 cm^{-1}, and the C–O band was red-shifted from 1099 to 1093 cm^{-1}. The peak at 1745 cm^{-1} was

assigned to the C=O stretching of carboxyl group. A strong peak centered at 2500 cm^{-1} was assigned to the O–D stretching band, and the peak at 1214 cm^{-1} was assigned to the δ(D–O–D) bending band. The redshift of O–D and blueshift of C−H stretching bands were detected with increasing D$_2$O content. The observed redshift of O−D might be attributed to the partial self-aggregation of water molecules. It can also be inferred that water content affected intermolecular interactions by forming multiple hydrogen bonds with PEG and OA.

3.2 Microemulsion formation of DES-based biphasic system

Xylose-to-furfural conversion is typically conducted at high temperatures and/or for long reaction time.[27] Under a typical reaction condition (150 ^{o}C, 60 min), degradation of certain DES components was observed, accompanied by the generation of formic acid, as detected via HPLC (Figure S1). In Figure 2a, adding NaCl solution in DES (D$_{42}$S$_{28}$) significantly alleviated the degradation of OA, decreasing its mass reduction from 50.0% to 21.5%. PEG was more stable in this system, showing minor loss (3.5%-7.7%). The partition of furfural in this biphasic system was investigated at a MIBK/DES (with water) ratio of 30:70, as shown in Figure 2b. Furfural solubility in the MIBK phase increased with the increase of water content in DES. Moreover, the addition of water and NaCl, particularly NaCl, increased the partition coefficient of furfural in the organic phase (Figure 2b).

Interestingly, the NaCl-containing biphasic system became emulsified upon vigorous agitation (Figure S2b) regardless of temperature and the emulsion remained stable with continuous agitation (Figure 2c-e). PEG, being amphiphilic, is commonly used as an emulsifier to prepare O/W emulsions.[28] Its emulsifiability was enhanced in the presence of NaCl. Salt microcrystals formed surrounding the micelles in emulsions (Figure 2d-e), increasing the contact areas between substrates and salt crystals. PEG introduced depletion interaction into the interphase of emulsion

droplets and sodium microcrystals. This attractive interaction facilitated the adsorption of sodium microcrystals onto the droplet surface and simultaneously suppressed desorption once adsorbed, inhibiting phase inversion as well as providing great stability.[29] Stabilized emulsion micelles could protect furfural from side reactions in acidic DES phase. Such emulsion system acted as microcarriers to confine MIBK in the aqueous phase, increasing the interfacial area and improving furfural extraction. The biphasic system was demulsified when sodium crystals settled without stirring. The saturated NaCl facilitated the phase separation of DES and MIBK (Figure 2c), promoting the furfural partition into organic phase.

3.3 Pretreatment effectiveness

The compositions and enzymatic digestibility of the pulp recovered from biphasic reaction system were analyzed to evaluate the fractionation effectiveness. Especially, the effects of NaCl content in reaction media were investigated under a representative reaction condition (150 ℃ for 60 min). The resulting pulp contained 71%-79% glucan, 14%-23% lignin but no xylan (Figure 3a). Lignin content in the pulp reached the highest (23%) when NaCl solution was 28% ($D_{42}S_{28}$, corresponding to 7% NaCl). The enzymatic digestibility of cellulose in the pulp ranged from 74.6% to 88.0% (Figure 3b). In general, pulp with lower lignin content tends to be more digestible due to the high accessibility to cellulase enzymes.[30] Surprisingly, the pulp containing the highest lignin content (23%) resulting from $D_{42}S_{28}$ treatment showed the highest enzymatic digestibility (88%) under the sub-optimal enzymatic hydrolysis condition. This could be attributed to the lignin modification by PEG during the fractionation, which subsequently reduced the non-productive cellulase adsorption.[31] The FTIR spectrum of pulp from $D_{42}S_{28}$ (Figure S3, with band assignments in Table S8) displayed C–O stretching vibration, possibly originating from PEG and/or OA, at 1104 cm^{-1}, suggesting modification of pulp and lignin by those DES constituents. The out-of-plane

bending vibrations of crystalline cellulose appeared at 777 and 721 cm^{-1}. In raw switchgrass, an out-of-plane bending vibration of C–H in lignin was observed at 986 cm^{-1}, but this band disappeared in the pulp. These indicated that the majority of lignin was removed during treatment, leaving cellulose exposed.

Increasing NaCl from 7% to 12.3-14% caused a decline in digestibility, even with lower lignin content. For example, the pulp resulting from $D_{56}S_{14}$ and $D_{14}S_{56}$ pretreatment, containing similar lignin and cellulose contents, showed different enzymatic digestibility (87.5% and 74.6%, respectively). High NaCl content in the $D_{14}S_{56}$ pretreatment promoted undesired reactions, resulting in the formation of pseudolignin and condensed lignin,[32] which in turn could deposit onto the surface of the cellulose, lowering the enzymatic hydrolysis efficiency. Moreover, the reduced PEG content in $D_{14}S_{56}$ treatment significantly decreased the lignin-PEG interactions. In short, this pretreatment system can separate cellulose and lignin with high efficiency, and it can also be inferred that high NaCl content induced negative modifications of pulp chemistry, directly influencing enzymatic hydrolysis, although delignification efficiency may not change noticeably.

3.4 Furfural production

Furfural formation simultaneously occurred during the pretreatment, which was further investigated under the reaction condition of 150 ºC for 60 min. The study on water effect showed that furfural yield was improved when using hydrated DES ($D_{63}W_7$, $D_{49}W_{21}$, and $D_{35}W_{35}$) for fractionation compared to using pure DES (D_{70}) in biphasic system (Figure 3c). The DES/MIBK system containing 21% water reached the highest furfural yield of 14.62%, while the biphasic system with 7% water content had the lowest yield. Compared to furfural production using pure DES, the use of hydrated DES resulted in almost up to 4-fold increase in yield. However, the furfural yields obtained under those conditions were still unsatisfying.

Impressively, replacing water with the same quantity of NaCl solution increased furfural yield more than 5 times under the same condition ($D_{49}W_{21}$ vs. $D_{49}S_{21}$). NaCl should play a dual role in the furfural production with improved yield. One role was to catalyze the xylose-to-furfural conversion as a metal chloride salt, similar to that reported in prior studies.[33] The other role was to facilitate the formation of microemulsion, which enhanced extraction of furfural into organic phase. The furfural yield increased with the increase in NaCl content and reached the highest yield of 76.5% at the presence of 12.3% NaCl. The furfural selectivity showed a similar trend, with the highest of 82.02% (Figure 3c). Both furfural yield and selectivity dropped with further increase in NaCl content. Excess NaCl reduces the acidity of the reaction medium, resulting in insufficient xylose conversion accompanied with increased side reaction associated with furfural degradation into humin. High water content in the biphasic system could also reduce its reactivity. As a result, xylose conversion decreased from 94.19% in $D_{28}S_{49}$ to 88.01% in $D_{14}S_{56}$ (Table S4) and furfural selectivity did not increase.

The effects of reaction time and temperature on furfural production were also studied (Figure 4). The complete xylose conversion along with the highest furfural yield was obtained when the reaction time for $D_{42}S_{28}$ was 80 min at 150 °C (Figure 4a). Prolonging the reaction time at the same temperature led to reduced furfural yield due to side reactions under server conditions, while shortening the reaction time to 60 min would be beneficial for furfural selectivity. The darkening color of the solid residue also suggested a severer reaction with prolonged time (Figure 4b). For the pretreatment using the same DES, increasing the temperature from 130 to 160 °C at a given time (60 min) favored the xylose dehydration into furfural with the higher yield, reaching the highest yield of 74.8% and selectivity of 74.9% at 160 °C (Figure 4c). Although $D_{42}S_{28}$ required a longer time or higher temperature to maximize furfural yields, it appeared to be less effective than $D_{49}S_{21}$ above discussed. These findings suggested an optimal condition for lignocellulose/xylan-

to-furfural in a single step can be DES-specific. On the other hand, properly increasing NaCl and water contents in the reaction media can boost the furfural production under less severe reaction conditions.

3.5 Lignin chemistry

2D HSQC NMR spectrum of PEG-*g*-lignin extracted from the biphasic reaction system ($D_{42}S_{28}$, 150 ºC, 60 min) revealed signals of main lignin inter-monomeric units and polymer chain end-units (Figure 5a and b), showing similar side chains and aromatic regions to cellulolytic enzyme lignin (CEL) of our previous study.[34] In Figure 5a, β-aryl ether unit (β-O-4, Aα), phenyl coumarin unit (β-5, Bα), and resinol unit (β-β, Cα) interlinkages were detected at δC/δH 71.32/4.89, 86.60/5.49, and 84.61/4.64 ppm. The β-position of β-β ($C_β$) signals was centered at 53.05/3.11 ppm. γ-position of β-5 ($B_γ$) and β-β ($C_γ$) were at 62.02/3.70, and 70.66/4.17 ppm, respectively. Compared to CEL, new signals assigned to α-PEG-β-O-4 units (A´) and substituted PEG chains (P) were recognized at 80.62/4.67 (A´α), 59.70/3.48 (P_1), 69.33/3.5 ($P_{3/4}$), 71.99/3.42 (P_2). A´$_γ$ of γ-acetylated β-O-4 linkage was detected at 59.70/3.64 ppm.[35] Volume integration analysis revealed that the β-O-4 interlinkage in the PEG-*g*-lignin accounted for 18.25%, β-5 for 0.37%, and β-β linkages for 2.44% (Table S5). The partial retention of β-O-4 in PEG-*g*-lignin compared with CEL (46.7%) suggested the dissociation of this interlinkage during the fractionation. According to the NMR spectrum, PEGylation occurred on the α-position of β-O-4 structure (A´ in Figure 5), converted α-OH-β-O-4 to α-PEG-β-O-4 linkage.[36] Thus, PEG was grafted onto the α-position of β-O-4 structure of lignin during the fractionation.

The main cross-signals in the aromatic region of PEG-*g*-lignin correspond to Syringyl (S), Guaiacyl (G), and *p*-Hydroxyphenyl (H) units. Compared with CEL,[34] PEG-*g*-lignin showed a shrinkage of contours for S and G units, and the S/G ratio of PEG-*g*-lignin (S/G=1.47) was higher

than that of CEL (S/G=0.7). Plausibly, the reduced intensity of S and G was due to the condensed structure formed during the fractionation process. Condensation at 2-, 5-, and 6-positions would make it lack of hydrogen signals in HSQC NMR.[34, 37] The increased S/G ratio suggested that lignin fragments rich in G-units tend to condense. Prominent signals corresponding to ferulate (FA) and *p*-Coumarate (*p*CA) were also detected in the aromatic region of PEG-*g*-lignin.[38] The cross-peak centered at δC/δH 129.84/7.45 ppm were attributed to *p*CA$_{2/6}$, and the correlation peak of *p*CA$_{3/5}$ overlapped with G5 around 114.91/6.72 ppm. The signal for FA$_2$ was observed around 110.91/7.27 ppm. The cross-peaks for vinyl carbons in *p*CA and FA structures overlapped around C$_8$/H$_8$ 113.56/6.25-6.32 ppm.

3.6 Proposed reaction mechanism

PEG-based DES successfully broke down most interlinkages in the lignocellulose complex in switchgrass. The possible mechanism for xylan to furfural was illustrated in Figure 6. OA acted as the primary acid catalyst, depolymerizing xylan by protonating the hydroxyl groups and facilitating the cleavage of glycosidic bonds. The depolymerization released xylose, which subsequently isomerized into 1,2-enediol under acidic conditions. NaCl, with its strong hydration effect compared to hydrogen ions (H$^+$), enhanced the acidity of the reaction medium by releasing and increasing the activity of free H$^+$.[39] The addition of NaCl significantly decreased the pH, resulting in the DES/NaCl mixture having a lower pH than either pure DES or NaCl solution (Table S6). The increased acidity further promoted the depolymerization of xylan and the isomerization of xylose. The presence of Cl$^-$, functioning as an electron donor in Lewis acid, facilitated the formation of 1,2-enediol. The subsequent H$^+$-catalyzed dehydration of 1,2-enediol led to cyclization and the formation of furfural.[40]

The furfural yield obtained under the optimized DES condition ($D_{21}S_{49}$, 150 ºC, 60 min) in this study were higher than those obtained from most reactions previously reported using lignocellulose as a substrate and even comparable to those using pure xylose (Table S7).[41, 42] A possible reason for this high furfural yield was the rapid reaction rate facilitated by Cl^- from metal chloride salt, which outpaced side reactions, resulting in enhanced furfural production. Another contributing factor could be the stabilization of emulsion micelles by recrystallized salts, primarily sodium chloride crystals, with the possible inclusion of sodium oxalate. Salt crystals appeared immediately by mixing PEG-based DES with NaCl solution. With mixing solvent diffusion occurred at the liquid-liquid interface, potentially forming $PEG-H_2O$ supramolecular complexes, causing supersaturation at the interfacial area and enabling crystal formation.[28, 43] In the meantime, oil-in-water (O/W) droplets were generated, and sodium salt crystals would provide nucleation sites to promote micelles formation.

Additionally, sodium salts were proven to reduce the electrostatic repulsion among the surfactant head groups, facilitating the self-aggregation of PEG and reducing the critical micelle concentration in emulsion.[44] Crystals were simultaneously adsorbed to the O/W micelle interface, helping to stabilize the O/W structure, which is the typical function of particles in Pickering emulsions.[45] The accumulation of salt crystals around the emulsion micelles resulted in concentrated free ions, including H^+, at the micellar interface. Given the noticeable catalytic effects of metal chloride salts, the main catalytic reactions likely occurred at the micelle interface. In the meantime, furfural was transferred to the organic phase of O/W micelle, driven by the PEG chains and salting-out effect of sodium salt, achieving efficient extraction while minimizing side reactions.

4. Conclusions

The polyethylene glycol (PEG):oxalic acid (OA) deep eutectic solvent (DES) based biphasic system demonstrates significant promise as a novel reaction system for biorefinery. Enhanced hydrogen bonding interactions improved the dissolution and pretreatment efficiency of DES, promoting effective fractionation of switchgrass. Xylan was selectively converted to furfural with NaCl as a catalyst, which reduced OA degradation, enhanced PEG stability, and improved furfural partitioning into the organic phase. The sodium salt crystals triggered the formation of O/W microemulsion, facilitating the continuous furfural conversion and extraction. Maximum furfural yield of 76.5% was achieved at the presence of 12.3% NaCl in the DES under the reaction condition of 150 ℃ and 60 min. The cellulose pulp had the highest enzymatic digestibility of 88% while containing 14-23% lignin. The extracted lignin showed PEG-functionalized motifs and partially preserved β-O-4 interlinkage. The proposed biphasic solvent system provides an efficient approach for biomass fractionation and simultaneous conversion of xylan to furfural via process intensification for maximizing biomass conversion.

Acknowledgments

Conflict of Interest

There is no conflict of interest to declare.

Associated Content

Supporting information: additional analysis and experimental section including quantitative analysis of 2D NMR spectrum of recovered lignin and enzymatic hydrolysis of pulp; detailed information of composition of biphasic solvent systems; additional results of thermal behavior,

Green Chemistry Accepted Manuscript

viscosity and acidity of DES; additional result of xylose conversion during fractionation; additional FTIR analysis of pulp; comparison of furfural production via different biphasic systems from biomass; additional experiment phenomenon of Pickering emulsion formation.

References

1.   J. J. Bozell and G. R. Petersen, *Green Chem.*, 2010, **12**, 539-554.

2.   C. M. Cai, T. Zhang, R. Kumar and C. E. Wyman, *J. Chem. Technol. Biotechnol.*, 2014, **89**, 2-10.

3.   L. Zhang, H. Yu, P. Wang, H. Dong and X. Peng, *Bioresour. Technol.*, 2013, **130**, 110-116.

4.   S. Peleteiro, S. Rivas, J. L. Alonso, V. Santos and J. C. Parajó, *Bioresour. Technol.*, 2016, **202**, 181-191.

5.   A. S. Mamman, J. M. Lee, Y. C. Kim, I. T. Hwang, N. J. Park, Y. K. Hwang, J. S. Chang and J. S. Hwang, *Biofuels, Bioprod. Biorefin.*, 2008, **2**, 438-454.

6.   Y. Chen, L. Fu, Z. Liu, F. Dai, Z. Dong, D. Li, H. Liu, D. Zhao and Y. Lou, *Journal of Molecular Liquids*, 2020, **318**, 114042.

7.   Y. Liu, N. Deak, Z. Wang, H. Yu, L. Hameleers, E. Jurak, P. J. Deuss and K. Barta, *Nature Communications*, 2021, **12**, 5424.

8.   B. Xue, Y. Yang, R. Tang, D. Xue, Y. Sun and X. Li, *International Journal of Biological Macromolecules*, 2020, **164**, 480-488.

9.   D. Xu, W. Tang, Z. Tang and Y. He, *Catalysts*, 2023, **13**, 467.

10.   J. Cheng, C. Huang, Y. Zhan, X. Liu, J. Wang, C. Huang, G. Fang, A. J. Ragauskas, Z. Xie and X. Meng, *Bioresource Technology*, 2023, **387**, 129653.

11.   E. Nzediegwu and M.-J. Dumont, *Cellulose*, 2023, **30**, 4957-4970.

Green Chemistry Accepted Manuscript

12.   G. A. D. Castro, R. C. Batista, R. d. C. S. de Sousa, A. d. C. O. Carneiro and S. A. Fernandes, *Reaction Chemistry & Engineering*, 2023, **8**, 1969-1980.

13.   M. Pera-Titus, L. Leclercq, J. M. Clacens, F. De Campo and V. Nardello-Rataj, *Angewandte Chemie International Edition*, 2015, **54**, 2006-2021.

14.   Z.-Q. Liu, J.-L. Guo, R.-H. Liang, F.-X. Wang, Z.-K. Li, Y. Liu and A. Ying, *Chemical Engineering Journal*, 2024, **479**, 147757.

15.   M. Jiang, J. Tan, Y. Chen, W. Zhang, P. Chen, Y. Tang and Q. Gao, *Chemical Communications*, 2023, **59**, 3103-3106.

16.   A. Sluiter, B. Hames, R. Ruiz, C. Scarlata, J. Sluiter, D. Templeton and D. Crocker, *Laboratory analytical procedure*, 2008, **1617**, 1-16.

17.   X.-D. Hou, A.-L. Li, K.-P. Lin, Y.-Y. Wang, Z.-Y. Kuang and S.-L. Cao, *Bioresource technology*, 2018, **249**, 261-267.

18.   E. L. Smith, A. P. Abbott and K. S. Ryder, *Chemical reviews*, 2014, **114**, 11060-11082.

19.   Z. Li and P. I. Lee, *International journal of pharmaceutics*, 2016, **505**, 283-288.

20.   M. Fronduti, T. Del Giacco, E. Rossi, M. Tiecco and R. Germani, *Journal of Molecular Liquids*, 2023, **379**, 121679.

21.   Q. Xia, Y. Liu, J. Meng, W. Cheng, W. Chen, S. Liu, Y. Liu, J. Li and H. Yu, *Green chemistry*, 2018, **20**, 2711-2721.

22.   A. K. Das, M. Sharma, D. Mondal and K. Prasad, *Carbohydrate polymers*, 2016, **136**, 930-935.

23.   X. Chang, Y. Zhang, X. Weng, P. Su, W. Wu and Y. Mo, *The Journal of Physical Chemistry A*, 2016, **120**, 2749-2756.

24.   Y. Yang, W. Zhang and X. Gao, *International journal of quantum chemistry*, 2006, **106**, 1199-1207.

Green Chemistry Accepted Manuscript

25.   Y. Gu, T. Kar and S. Scheiner, *Journal of the American Chemical Society*, 1999, **121**, 9411-9422.

26.   K. D. O. Vigier, G. Chatel and F. Jérôme, *ChemCatChem*, 2015, **7**, 1250-1260.

27.   A. Jaswal, P. P. Singh and T. Mondal, *Green Chemistry*, 2022, **24**, 510-551.

28.   Z. Wang, J. Song, S. Zhang, X.-Q. Xu and Y. Wang, *Langmuir*, 2017, **33**, 9160-9169.

29.   K. Kim, S. Kim, J. Ryu, J. Jeon, S. G. Jang, H. Kim, D.-G. Gweon, W. B. Im, Y. Han and H. Kim, *Nature Communications*, 2017, **8**, 14305.

30.   M. Takada, R. Chandra, J. Wu and J. N. Saddler, *Bioresource Technology*, 2020, **302**, 122895.

31.   C. Lai, Y. Jia, C. Yang, L. Chen, H. Shi and Q. Yong, *ACS Sustainable Chemistry & Engineering*, 2020, **8**, 1797-1804.

32.   C. Huang, W. Lin, Y. Zheng, X. Zhao, A. Ragauskas and X. Meng, *Green Chemistry*, 2022, **24**, 5263-5279.

33.   N. Zhou, C. Zhang, Y. Cao, J. Zhan, J. Fan, J. H. Clark and S. Zhang, *Journal of Cleaner Production*, 2021, **311**, 127780.

34.   Z. Chen, X. Bai, L. A, H. Zhang and C. Wan, *ACS Sustainable Chemistry & Engineering*, 2020, **8**, 9783-9793.

35.   J. Cheng, X. Liu, Y. Zhan, J. Wang, X. Meng, X. Zhou, C. Geun Yoo, C. Huang, C. Huang and G. Fang, *ChemSusChem*, 2023, e202301161.

36.   T. T. Nge, Y. Tobimatsu, S. Takahashi, E. Takata, M. Yamamura, Y. Miyagawa, T. Ikeda, T. Umezawa and T. Yamada, *ACS Sustainable Chemistry & Engineering*, 2018, **6**, 7841-7848.

37.   J.-L. Wen, T.-Q. Yuan, S.-L. Sun, F. Xu and R.-C. Sun, *Green Chemistry*, 2014, **16**, 181-190.

38.   J. C. del Río, J. Rencoret, G. Marques, A. Gutiérrez, D. Ibarra, J. I. Santos, J. Jiménez-Barbero, L. Zhang and Á. T. Martínez, *Journal of Agricultural and Food Chemistry*, 2008, **56**, 9525-9534.

39.   F. E. Critchfield and J. B. Johnson, *Analytical Chemistry*, 1959, **31**, 570-572.

40.   J. N. M. Soetedjo, C. B. Rasrendra and H. J. Heeres, *IOP Conference Series: Materials Science and Engineering*, 2020, **742**, 012049.

41.   D. M. E. Delgadillo, G. A. D. Castro and S. A. Fernandes, *Reaction Chemistry & Engineering*, 2024.

42.   S. Wang, Y. Zhao, H. Lin, J. Chen, L. Zhu and Z. Luo, *Green chemistry*, 2017, **19**, 3869-3879.

43.   W. Zhang, Y. Zhu, X. Liu, D. Wang, J. Li, L. Jiang and J. Jin, *Angewandte Chemie International Edition*, 2014, **53**, 856-860.

44.   S. Aktar, M. Saha, S. Mahbub, M. A. Halim, M. A. Rub, M. A. Hoque, D. S. Islam, D. Kumar, Y. G. Alghamdi and A. M. Asiri, *Journal of Molecular Liquids*, 2020, **306**, 112880.

45.   S. Ghosh and D. Rousseau, *Current opinion in colloid & interface science*, 2011, **16**, 421-431.
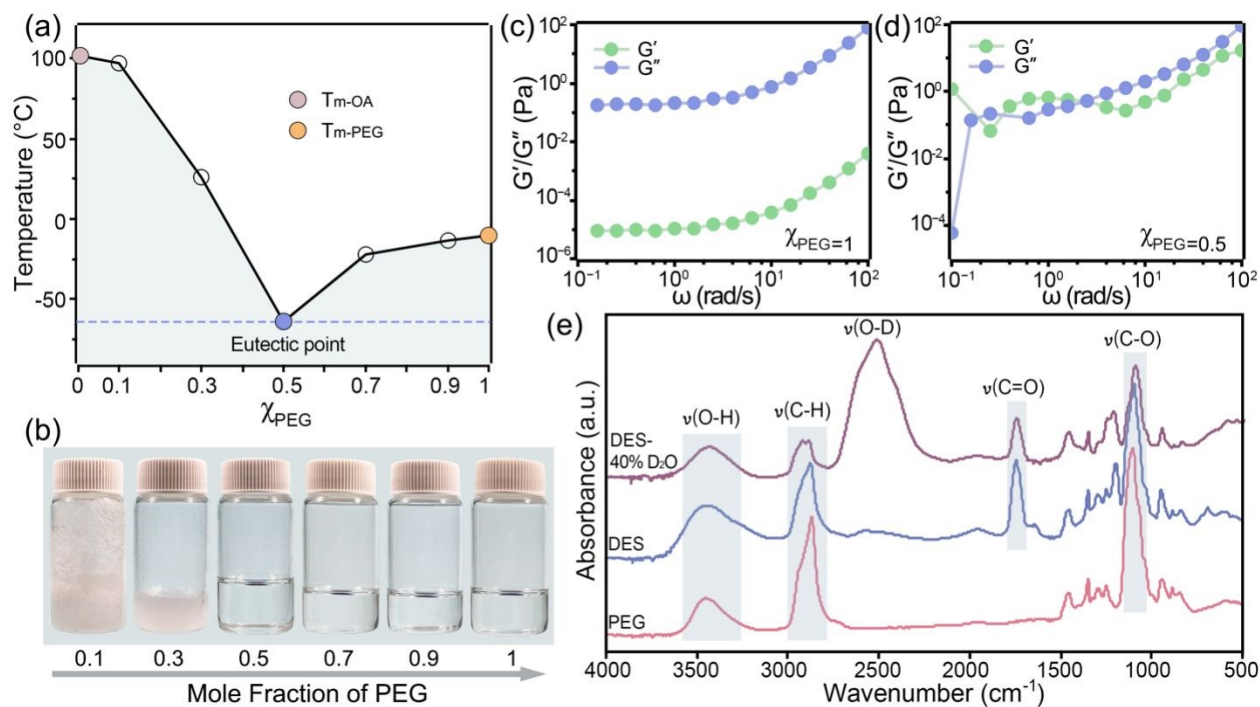
Figure captions

Figure 1. DES property and structure. (a) Phase diagram of PEG:OA binary DES: $T_{m\text{-}OA}$ and $T_{m\text{-}PEG}$ are the melting points of OA and PEG, respectively; blue dashed line is the eutectic temperature; χ_{PEG} is the mole fraction of PEG in DES. (b) Photos of DES samples with varied χ_{PEG}. (c) and (d) Viscoelasticity behaviors of pure PEG (χ_{PEG}=1) and DES (χ_{PEG}=0.5), respectively. (e) FTIR spectra of PEG, DES (χ_{PEG}=0.5), and DES (χ_{PEG}=0.5) containing 40% D_2O.
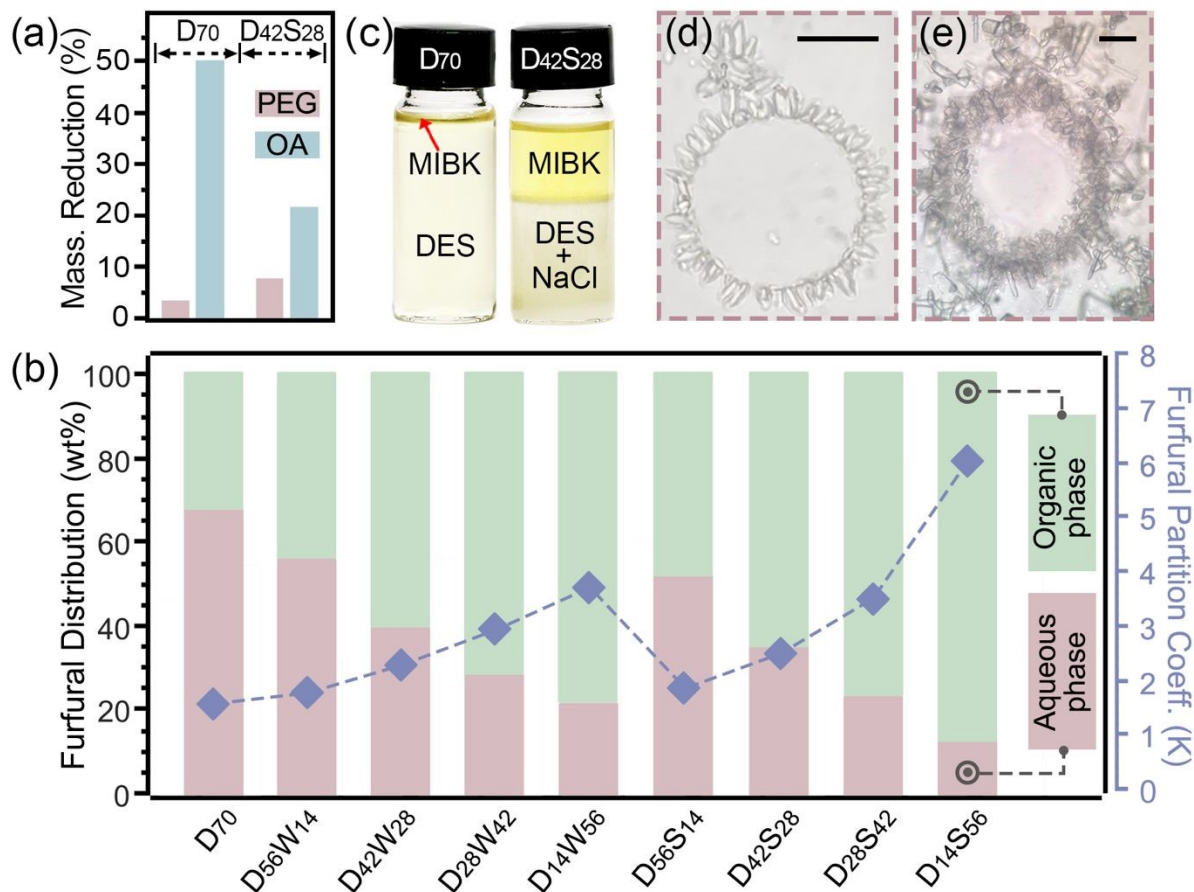
Figure 2. NaCl effect on DES-MIBK biphasic solvent. (a) Thermal stability (mass reduction percentage) of DES constituents after heating at 150 ºC for 60 min. (b) Furfural distribution percentage (stacked bar chart) and partition coefficients (K, line chart) in the biphasic system at room temperature (25 ± 1 ºC). (c) Photos of cooled biphasic solvent after heating at 150 ºC for 60 min. Micrographs of micelle in emulsion at (d) room temperature (25 ± 1 ºC) and (e) after heated at 150 ºC for 60 min (scale bars: 15 μm).

Figure 3. Effect of NaCl content on the pulp quality and furfural production. (a) Component percentage of pulp, (b) enzymatic digestibility of pulp, (c) furfural yield and selectivity.

Figure 4. Effect of reaction time and temperature. (a) Furfural yield, furfural selectivity and xylose conversion at 150 ºC with varied times, (b) photos of solid residues obtained at 150 ºC with varied times, (c) furfural yield, furfural selectivity and xylose conversion at 60 min with varied temperatures.

Figure 5. 2D HSQC NMR spectra of PEG-*g*-lignin obtained from biphasic fractionation process. (a) side-chain region (δC/δH 90~50/6.0~2.75), (b) aromatic region (δC/δH 135~100/8.0~6.0).

Figure 6. Schematic diagram of lignocellulose fractionation and interfacial catalysis for furfural formation.

Figure 1. DES property and structure. (a) Phase diagram of PEG:OA binary DES: T_{m-OA} and T_{m-PEG} are the melting points of OA and PEG, respectively; blue dashed line is the eutectic temperature; χ_{PEG} is the mole fraction of PEG in DES. (b) Photos of DESs with varied χ_{PEG}. (c) and (d) Viscoelasticity behaviors of pure PEG (χ_{PEG}=1) and DES (χ_{PEG}=0.5), respectively. (e) FTIR spectra of PEG, DES (χ_{PEG}=0.5), and DES (χ_{PEG}=0.5) containing 40% D_2O.

Figure 2. NaCl effect on DES-MIBK biphasic solvent. (a) Thermal stability (mass reduction percentage) of DES constituents after heating at 150 ºC for 60 min. (b) Furfural distribution percentage (stacked bar chart) and partition coefficients (K, line chart) in the biphasic system at room temperature (25 ± 1 ºC). (c) Photos of cooled biphasic solvent after heating at 150 ºC for 60 min. Micrographs of micelle in emulsion at (d) room temperature (25 ± 1 ºC) and (e) after heated at 150 ºC for 60 min (scale bars: 15 μm).

Figure 3. Effect of NaCl content on the pulp quality and furfural production. (a) Component percentage of pulp, (b) enzymatic digestibility of pulp, (c) furfural yield and selectivity.
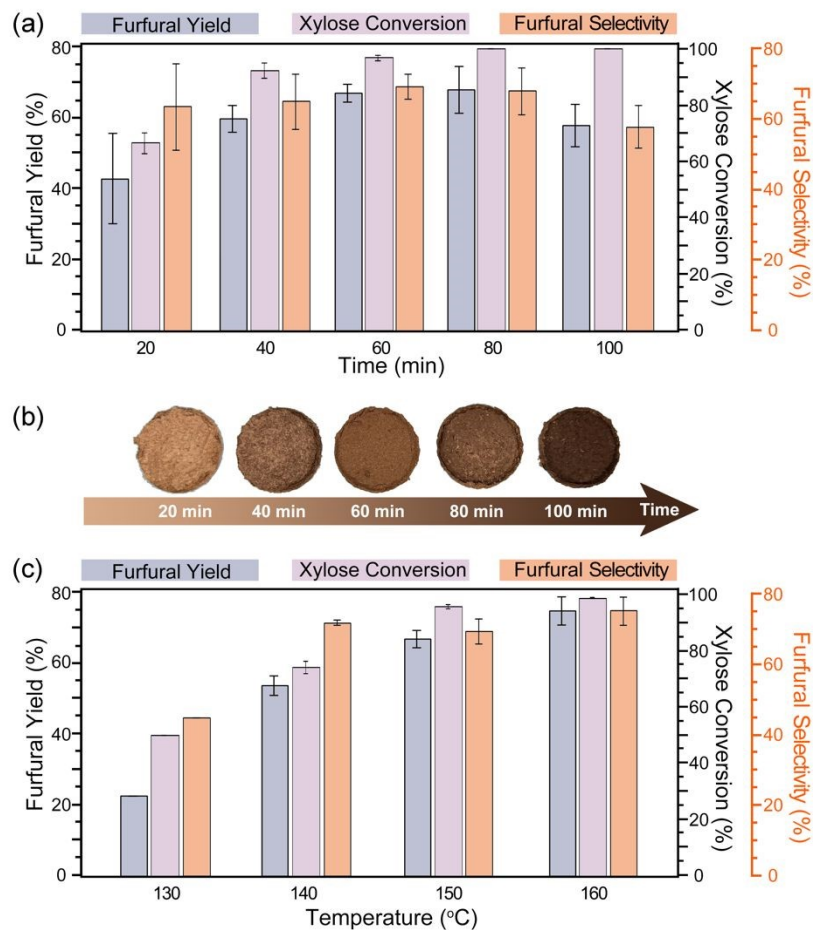
Figure 4. Effect of reaction time and temperature. (a) Furfural yield, furfural selectivity and xylose conversion at 150 ºC with varied times, (b) photos of solid residues obtained at 150 ºC with varied times, (c) furfural yield, furfural selectivity and xylose conversion at 60 min with varied temperatures.
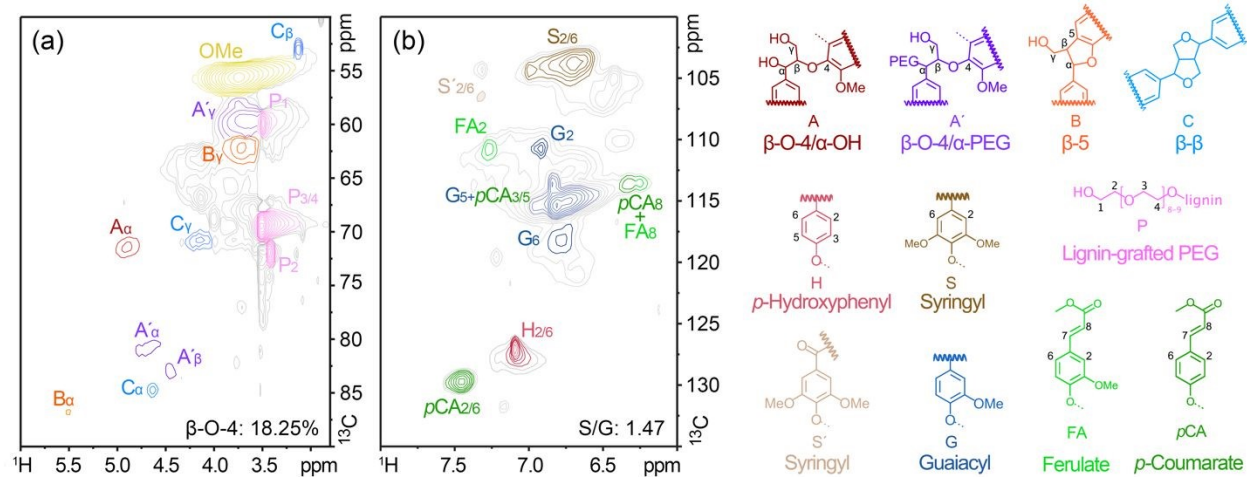
Figure 5. 2D HSQC NMR spectra of PEG-*g*-lignin obtained from biphasic fractionation process.

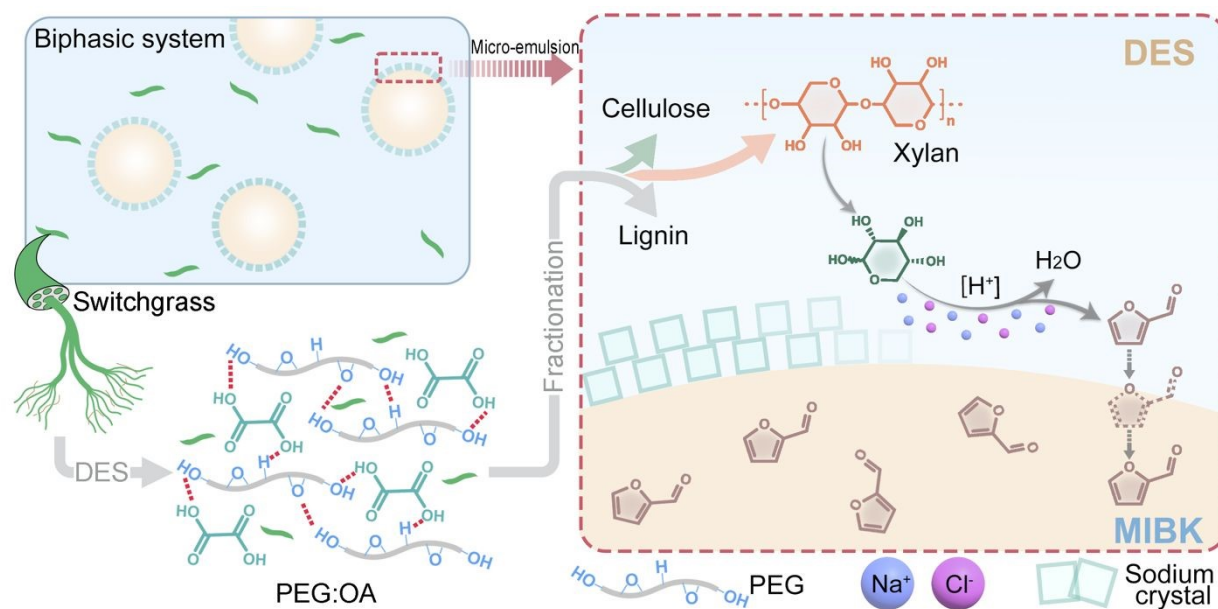(a) side-chain region (δC/δH 90~50/6.0~2.75), (b) aromatic region (δC/δH 135~100/8.0~6.0).

Figure 6. Schematic diagram of lignocellulose fractionation and interfacial catalysis for furfural formation.

The authors confirm that the data supporting the findings of this study are available within the article and its supplementary materials.